Contact strength of solids with periodic relief under partial frictional slip

I.G. Goryacheva [1,a], N.I. Malanchuk [2,b], R.M. Martynyak [2,b], and K.A. Chumak [2,b]

[1] Institute for Problems in Mechanics, Russian Academy of Sciences,
Vernadskogo pr. 101, Moskow, Russia

[2] Pidstryhach Institute for Applied Problems of Mechanics and Mathematics,
National Academy of Sciences of Ukraine, Naukova 3-b, Lviv, Ukraine

[a] goryache@ipmnet.ru, [b] labmtd@iapmm.lviv.ua

Keywords: stick-slip contact, periodic relief, groove, contact strength.

Abstract. The contact interaction of two elastic solids of identical materials, one of which has a regular relief that is formed by a periodic system of shallow tunnel grooves of the same shape, under sequential loading by normal and shear forces is studied. By using the complex potential method, the corresponding problem is reduced to a singular integral equation with Hilbert kernel for the relative tangential shift of boundaries. The analytical solution to the problem is obtained for a certain shape of the groove. By making use of the obtained analytical solution, the surface principal normal and shear stresses along with the parameters of slip zones and their dependences on the loading are analyzed. The most possible regions of the cracks initiation and plastic yielding is found on the basis of the classical strength criteria.

Introduction. There are different ways of processing and modification of the mating surfaces to improve the functional characteristics of a moving connection and to create the sites with predictable contact behavior. In recent years, micro-texturing of surfaces is efficiently used [1]. This approach consists in formation of periodically located grooves of the same shape. To create such microgeometry, the laser beam processing is commonly used. The contact parameters of micro-textured bodies along with their contact strength, stiffness, and wear can be predicted on the basis of analytical or analytical-numerical solutions of contact problems for surfaces with periodic systems of grooves and pits by taking into account the friction, stick, and slip.

The present paper concerns the two-dimensional contact problem of frictional interaction between two elastic half-spaces with periodical relief of the surfaces under the sequential loading by normal and shear forces. The aim of the work is to examine the behavior of the contacting solids and assess the strength of the contacting couple. In our investigation we obtain analytical solution. The knowledge of the analytical solutions to contact problems serves as a ground for the investigation of strength, durability, fatigue of contacting couples. Much attention has been given to the interaction of solids with regular relief (a wavy surface or a relief formed by the periodic system of indenters) in the case of frictionless (see [2–5]) and frictional sliding (see [6–10]) contact of such bodies. No attention, however, has been given to the contact interaction of bodies with textured surfaces when periodic zones of local frictional slip arise.

Description of the problem. We investigate the contact interaction between two semi-infinite isotropic elastic solids D_1 and D_2 made of identical materials (bodies has identical Poisson's ratio $\nu_1 = \nu_2 = \nu$ and the shear modulus $G_1 = G_2 = G$) in the Cartesian coordinate system Oxy. The solid D_2 has a plane boundary. The boundary of D_1 is described by the periodic smooth function

$$r(x)=r(x+kd)=-r_0\left(1-\mathrm{tg}^2\frac{\pi x}{d}\Big/\mathrm{tg}^2\frac{\pi b}{d}\right)^{3/2},\ x\in[-b+kd,b+kd],\ k=0,\pm1,\pm2,\dots, \tag{1}$$

where $0<r_0/b<<1$, r_0 is the maximal depth of the grooves and d is the period. The maximum depth of the grooves r_0 is achieved in their center ($\max|r(x)|=r_0=|r(0+kd)|$) and $r(\pm b+kd)=r'(\pm b+kd)=0$. The bodies before contact are shown in Fig. 1.

Initially, the bodies are pressed by monotonically increasing nominal pressure p_n that leads to monotonic decrease in intercontact gaps size. Depending on value of p_n, either an incomplete contact of bodies (if $p_n<p_{cls}$) can be realized, when an intercontact gap will be within each groove, or a complete contact can be realized (if $p_n\geq p_{cls}$). Here p_{cls} is a nominal pressure at which the gaps will close completely and all points of the both surfaces will be in contact. We consider the situation when $p_n\geq p_{cls}$. Then, the bodies are subjected to the nominal tangential stress q_n (Fig. 2). According to the Amonton-Coulomb law, the bodies are in stick in each point of the contact region if the tangential contact stresses $q(x)=\tau_{xy}(x,0)$ are less than the product of the contact pressure $p(x)=-\sigma(x,0)$ and the friction coefficient μ: $q(x)<\mu p(x)$. So, the bodies are in stick if the inequality $q_n<\mu(p_n-p_{cls})$ is satisfied. If the nominal tangential stress q_n reaches the critical value $q_0=\mu(p_n-p_{cls})$, sliding starts in the central point of each groove. For the nominal tangential stress q_n from the range $q_0<q_n<\mu p_n$, the slip zones are arising within each groove beginning from its center, where the contact pressure reaches its minimum ($\min p(x)=p(0+kd)=p_n-p_{cls}$, $k=0,\pm1,\pm2,\dots$). The tangential stress $q(x)=\mu p(x)$ caused by the friction forces arises in the slip zones.

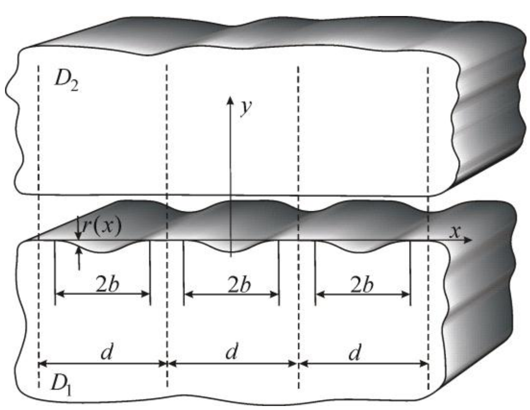

Fig. 1.

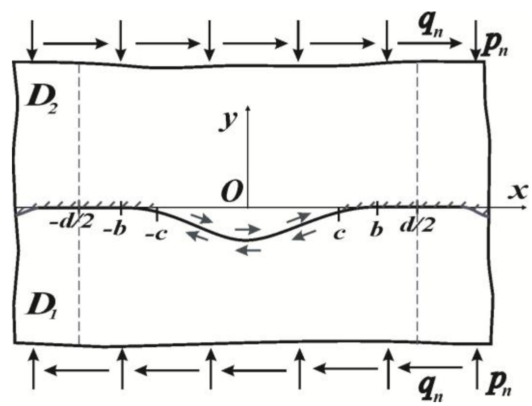

Fig.2.

In Fig. 2 the stick zones of surfaces are shaded. The direction of the sliding of the surfaces in the slip zones is indicated by arrows.

If the nominal tangential stress q_n reaches the value μp_n, the bodies are sliding throughout the contact surface. In this article we consider the tangential stress q_n from the range $q_0<q_n<\mu p_n$, which leads to appearance of the slip zone of width $2c$ within the each groove. The bodies are in stick beyond the slip zones.

Let us denote $I_k^w=[-w+kd,w+kd]$, $J_k^w=[-d/2+kd,\,-w+kd]\cup[w+kd,\,d/2+kd]$; $w=b,c$; and $J_k^{b,c}=[-b+kd,-c+kd]\cup[c+kd,b+kd]$. Here and further on, $k=0,\pm1,\pm2,\dots$

Under the above assumptions, the boundary conditions of the periodic contact problem are the following:

$$\sigma_y^-(x,0)=\sigma_y^+(x,0),\ \tau_{xy}^-(x,0)=\tau_{xy}^+(x,0),\ v^-(x,0)-v^+(x,0)=-r(x)\,; \tag{2}$$

$$\tau_{xy}^-(x,0)=-\mu\sigma_y^-(x,0) \tag{3}$$

in the slip zones ($x\in I_k^c$);

$$\sigma_y^-(x,0)=\sigma_y^+(x,0),\ \tau_{xy}^-(x,0)=\tau_{xy}^+(x,0)\,;$$

$$u^-(x,0)=u^+(x,0)\,,\ v^-(x,0)-v^+(x,0)=-r(x) \tag{4}$$

in the stick zones ($x\in J_k^c$);

$$\sigma_y=-p_n,\ \tau_{xy}=q_n,\ \sigma_x=0 \tag{5}$$

at infinity.

Hereinafter u and v are the components of the displacement-vector; σ_y, σ_x, and τ_{xy} are the stress-tensor components; superscripts "+" and "-" denote the limit values of functions at the interface in D_2 and D_1, respectively.

The problem under consideration lies in the determination of the width of the slip zones and the stress-strain state in the solids. In order to analyze the contact strength of the contact pair, much attention is paid to the distribution of the surface principal shear and normal stresses.

Solution of the problem. Let us present the stresses and derivatives of displacements in terms of the complex potentials in the form guaranteeing the satisfaction of the conditions (5)

$$\sigma_x+\sigma_y=4\operatorname{Re}\left[\Phi_l(z)\right]-p_n,\quad \sigma_y-i\tau_{xy}=\Phi_l(z)-\Phi_l(\bar z)+(z-\bar z)\overline{\Phi_l'(z)}-p_n-iq_n\,;$$

$$2G\left(u'+iv'\right)=\kappa\Phi_l(z)+\Phi_l(\bar z)-(z-\bar z)\overline{\Phi_l'(z)}+\frac{3-\kappa}{4}p_n,\ z\in D_l,\ l=1,2\,, \tag{6}$$

where $z=x+iy$, $i=\sqrt{-1}$, $\kappa=3-4\nu$, and $\Phi_1(z)$ and $\Phi_2(z)$ denote piecewise-analytic functions vanishing at infinity ($\Phi_1(\infty)=\Phi_2(\infty)=0$).

We define the complex potentials $\Phi_1(z)$ and $\Phi_2(z)$ through the functions of the grooves height $r(x)$ and the relative tangential shift of boundaries $U(x)=u^-(x,0)-u^+(x,0)$ in the slip zones $x\in I_k^c$

$$\Phi_1(z)=-\Phi_2(z)=\frac{(-1)^l G}{\pi i(1+\kappa)}\sum_{k=-\infty}^{\infty}\left\{\int_{-c+kd}^{c+kd}\frac{U'(t)dt}{t-z}-i\int_{-b+kd}^{b+kd}\frac{r'(t)dt}{t-z}\right\},\ z\in D_l,\ l=1,2\,. \tag{7}$$

Taking into account the periodicity of the functions $U(x)$ and $r(x)$, we can write

$$\Phi_1(z)=-\Phi_2(z)=\frac{(-1)^l G}{di(1+\kappa)}\left(\int_{-c}^{c}U'(t)\operatorname{ctg}\frac{\pi(t-z)}{d}dt-i\int_{-b}^{b}r'(t)\operatorname{ctg}\frac{\pi(t-z)}{d}dt\right),\ z\in D_l,\ l=1,2\,. \tag{8}$$

By substitution of the formulas (8) into the expressions (6), we find the contact pressure and tangential contact stress

$$p(x)=-\frac{2G}{d(1+\kappa)}\int_{-b}^{b} r'(t)\operatorname{ctg}\frac{\pi(t-x)}{d}dt+p_n,\; q(x)=-\frac{2G}{d(1+\kappa)}\int_{-c}^{c} U'(t)\operatorname{ctg}\frac{\pi(t-x)}{d}dt+q_n. \tag{9}$$

Substitution of the expressions (9) into the boundary condition (3) yields a singular integral equation (SIE) with Hilbert kernel for the function $U'(x)$

$$\int_{-c}^{c} U'(t)\operatorname{ctg}\frac{\pi(t-x)}{d}dt=\frac{d(1+\kappa)}{2G}(q_n-\mu p_n)+\mu\int_{-b}^{b} r'(t)\operatorname{ctg}\frac{\pi(t-x)}{d}dt,\; |x|\le c. \tag{10}$$

The function $U(x)$, taking into account its physical meaning, meets the following conditions:

$$U(-c+kd)=0,\; U(c+kd)=0,\; U'(-c+kd)=0,\; U'(c+kd)=0. \tag{11}$$

The first two conditions in (11) follow from the continuity of the tangential displacements of the boundaries, and the second two conditions in (11) provide boundedness of the tangential stress at the edges of the slip zones.

Let us introduce the variables $\xi=\operatorname{tg}(\pi x/d)$, $\eta=\operatorname{tg}(\pi t/d)$, by use of which the SIE with the Hilbert kernel (10) can be transformed into a SIE with the Cauchy kernel

$$\int_{-\alpha}^{\alpha}\frac{U'(\eta)}{\eta-\xi}d\eta=\frac{d(1+\kappa)(q_n-\mu p_n)}{2G(1+\xi^2)}+\mu\int_{-\gamma}^{\gamma}\frac{r'(\eta)}{\eta-\xi}d\eta,\; |\xi|\le\alpha,\; \alpha=\operatorname{tg}\frac{\pi c}{d},\; \gamma=\operatorname{tg}\frac{\pi b}{d}. \tag{12}$$

The conditions (11) in the new variables have the following form:

$$U(-\alpha)=0,\; U(\alpha)=0,\; U'(-\alpha)=0,\; U'(\alpha)=0. \tag{13}$$

In view of the second two conditions in (13), we find the solution of the SIE (12) bounded at the points $\xi=\pm\alpha$. Integration of this solution accounting for the first condition in (13) gives the relative tangential shift of boundaries, which in the original variables has the form [11]:

$$\begin{aligned}U(x)=&\frac{-\mu r_0}{\operatorname{tg}^3(\pi b/d)}\left(\operatorname{tg}^2\left(\frac{\pi c}{d}\right)-\operatorname{tg}^2\left(\frac{\pi x}{d}\right)\right)^{3/2}+\frac{d(1+\kappa)(q_n-\mu p_n)}{2G\pi}\left(\frac{\sqrt{\operatorname{tg}^2(\pi c/d)-\operatorname{tg}^2(\pi x/d)}}{\sqrt{1+\operatorname{tg}^2(\pi c/d)}}\right.\\&\left.-\frac{1}{2}\ln\left|\frac{\sqrt{1+\operatorname{tg}^2(\pi c/d)}+\sqrt{\operatorname{tg}^2(\pi c/d)-\operatorname{tg}^2(\pi x/d)}}{\sqrt{1+\operatorname{tg}^2(\pi c/d)}-\sqrt{\operatorname{tg}^2(\pi c/d)-\operatorname{tg}^2(\pi x/d)}}\right|\right),\quad x\in I_k^c,\quad c\le b.\end{aligned} \tag{14}$$

It should be noted that the bounded solution of the Eq. (12) exists if the RHS of (12) satisfies the additional condition [11], from which we obtain the equation for finding the slip zones width c:

$$\frac{d(1+\kappa)(q_n-\mu p_n)}{\pi G}\cos\frac{\pi c}{d}+\frac{3\mu r_0}{\operatorname{tg}(\pi b/d)}\left(1-\frac{\operatorname{tg}^2(\pi c/d)}{\operatorname{tg}^2(\pi b/d)}\right)=0.$$

By substitution the Eqs. (1) and (14) into the expressions (9), we obtain the contact stresses:

$$\sigma_y(x,0)=-p(x)=-\frac{6Gr_0\pi(1+\operatorname{tg}^2(\pi x/d))}{d(1+\kappa)\operatorname{tg}(\pi b/d)}\left(\frac{\operatorname{tg}^2(\pi x/d)}{\operatorname{tg}^2(\pi b/d)}-\frac{1}{2}\right)-p_n,\; x\in I_k^b,$$

$$\sigma_y(x,0)=\frac{6Gr_0\pi(1+\mathrm{tg}^2(\pi x/d))}{d(1+\kappa)\,\mathrm{tg}(\pi b/d)}\left(\left|\frac{\mathrm{tg}(\pi x/d)}{\mathrm{tg}(\pi b/d)}\right|\sqrt{\frac{\mathrm{tg}^2(\pi x/d)}{\mathrm{tg}^2(\pi b/d)}-1}-\frac{\mathrm{tg}^2(\pi x/d)}{\mathrm{tg}^2(\pi b/d)}+\frac{1}{2}\right)-p_n,\ x\in J_k^b, \qquad (15)$$

$$\sigma_x(x,0)=\frac{4G\pi\left(1+\mathrm{tg}^2(\pi x/d)\right)}{d(1+\kappa)}\,\mathrm{tg}\left(\frac{\pi x}{d}\right)\sqrt{\mathrm{tg}^2\left(\frac{\pi c}{d}\right)-\mathrm{tg}^2\left(\frac{\pi x}{d}\right)}\left(\frac{3\mu r_0}{\mathrm{tg}^3(\pi b/d)}+\right.$$

$$\left.+\frac{d(1+\kappa)(q_n-\mu p_n)\cos^2(\pi c/d)}{2G\pi\left(1+\mathrm{tg}^2(\pi x/d)\right)}\right)+\frac{6Gr_0\pi\left(1+\mathrm{tg}^2(\pi x/d)\right)}{d(1+\kappa)\,\mathrm{tg}(\pi b/d)}\left(\frac{1}{2}-\frac{\mathrm{tg}^2(\pi x/d)}{\mathrm{tg}^2(\pi b/d)}\right),\ x\in I_k^c,$$

$$\sigma_x(x,0)=\frac{6Gr_0\pi\left(1+\mathrm{tg}^2(\pi x/d)\right)}{d(1+\kappa)\,\mathrm{tg}(\pi b/d)}\left(\frac{1}{2}-\frac{\mathrm{tg}^2(\pi x/d)}{\mathrm{tg}^2(\pi b/d)}\right),\ x\in J_k^{b,c},$$

$$\sigma_x(x,0)=\frac{6Gr_0\pi\left(1+\mathrm{tg}^2(\pi x/d)\right)}{d(1+\kappa)\,\mathrm{tg}(\pi b/d)}\left(\left|\frac{\mathrm{tg}(\pi x/d)}{\mathrm{tg}(\pi b/d)}\right|\sqrt{\frac{\mathrm{tg}^2(\pi x/d)}{\mathrm{tg}^2(\pi b/d)}-1}-\frac{\mathrm{tg}^2(\pi x/d)}{\mathrm{tg}^2(\pi b/d)}+\frac{1}{2}\right),\ x\in J_k^b, \qquad (16)$$

$$\tau_{xy}(x,0)=q(x)=\frac{6Gr_0\pi\mu(1+\mathrm{tg}^2(\pi x/d))}{d(1+\kappa)\,\mathrm{tg}(\pi b/d)}\left(\frac{\mathrm{tg}^2(\pi x/d)}{\mathrm{tg}^2(\pi b/d)}-\frac{1}{2}\right)+\mu p_n,\ x\in I_k^c,$$

$$\tau_{xy}(x,0)=\frac{6Gr_0\pi\mu(1+\mathrm{tg}^2(\pi x/d))}{d(1+\kappa)\,\mathrm{tg}(\pi b/d)}\left(\frac{\mathrm{tg}^2(\pi x/d)}{\mathrm{tg}^2(\pi b/d)}-\frac{1}{2}\right)+\mu p_n-\frac{6Gr_0\pi\mu}{d(1+\kappa)\,\mathrm{tg}(\pi b/d)}\times$$

$$\times\left|\frac{\mathrm{tg}(\pi x/d)}{\mathrm{tg}(\pi b/d)}\right|\sqrt{\frac{\mathrm{tg}^2(\pi x/d)}{\mathrm{tg}^2(\pi b/d)}-\frac{\mathrm{tg}^2(\pi c/d)}{\mathrm{tg}^2(\pi b/d)}}\left(1+\mathrm{tg}^2\left(\frac{\pi x}{d}\right)+\frac{\mathrm{tg}^2(\pi c/d)-\mathrm{tg}^2(\pi b/d)}{2}\right),\ x\in J_k^c. \qquad (17)$$

Contact strength. The manufacture and operation of machine joints and construction units is accompanied by the appearance of various defects on their surfaces, in particular microcracks. This leads to the fact that the failure of the contacting bodies commonly begins on their surfaces. Hence, the effect of frictional slip on the surface strength of the textured bodies is analyzed below.

The strength of a body of a plastic material will be estimated with accordance to the third classical strength theory, and the strength of a body of a brittle material will be estimated with accordance to the first classical strength theory. According to the first strength theory, the principal stress has the determining influence on the strength of a body. The condition of the material failure is the condition that the principal normal stress σ_1 reaches or exceeds the ultimate tensile strength σ_t, or the condition that the principal normal stress σ_2 reaches or exceeds the ultimate compressive strength σ_c. The first strength theory may be used to predict the failure of a number of brittle materials – iron, steel, glass, stone, ceramics, etc. The third classical theory is commonly applied to assess the strength of plastic materials (copper, brass, lead, etc.). This theory assumes that a materials fails when the principal tangential stress $\tau_{\max}$ reaches the yields strength τ_*.

Using the Eqs. (15)–(17) and the formulas $\tau_{\max}=\sqrt{(\sigma_y-\sigma_x)^2/4+\tau_{xy}^2}$, $\sigma_1=(\sigma_x+\sigma_y)/2+\tau_{\max}$, $\sigma_2=(\sigma_x+\sigma_y)/2-\tau_{\max}$, we find the principal shear stress $\tau_{\max}$ and principal normal stresses σ_1, σ_2 on the surface of the body D_1:

$$\tau_{\max}(x,0)=\left(\left(\frac{p_n}{2}+\frac{2G\pi\left(1+\mathrm{tg}^2(\pi x/d)\right)}{d(1+\kappa)}\mathrm{tg}\left(\frac{\pi x}{d}\right)\sqrt{\mathrm{tg}^2\left(\frac{\pi c}{d}\right)-\mathrm{tg}^2\left(\frac{\pi x}{d}\right)}\left(\frac{3r_0\mu}{\mathrm{tg}^3(\pi b/d)}+\right.\right.\right.$$

$$\left.\left.\left.+\frac{d(1+\kappa)(q_n-\mu p_n)}{2G\pi\left(1+\mathrm{tg}^2(\pi x/d)\right)}\cos\frac{\pi c}{d}\right)\right)^2+\left(\frac{6Gr_0\pi\mu(1+\mathrm{tg}^2(\pi x/d))}{d(1+\kappa)\,\mathrm{tg}(\pi b/d)}\left(\frac{\mathrm{tg}^2(\pi x/d)}{\mathrm{tg}^2(\pi b/d)}-\frac{1}{2}\right)+\mu p_n\right)^2\right)^{1/2},\quad x\in I_k^c,$$

$$\tau_{\max}(x,0)=\left(\frac{p_n^2}{4}+\left(\frac{6Gr_0\pi\mu(1+\mathrm{tg}^2(\pi x/d))}{d(1+\kappa)\,\mathrm{tg}(\pi b/d)}\left(\frac{\mathrm{tg}^2(\pi x/d)}{\mathrm{tg}^2(\pi b/d)}-\frac{1}{2}\right)+\mu p_n-\frac{6Gr_0\pi\mu}{d(1+\kappa)\,\mathrm{tg}(\pi b/d)}\times\right.\right.$$

$$\left.\left.\times\left|\frac{\mathrm{tg}(\pi x/d)}{\mathrm{tg}(\pi b/d)}\right|\sqrt{\frac{\mathrm{tg}^2(\pi x/d)}{\mathrm{tg}^2(\pi b/d)}-\frac{\mathrm{tg}^2(\pi c/d)}{\mathrm{tg}^2(\pi b/d)}}\left(1+\mathrm{tg}^2\left(\frac{\pi x}{d}\right)+\frac{\mathrm{tg}^2(\pi c/d)-\mathrm{tg}^2(\pi b/d)}{2}\right)\right)^2\right)^{1/2},\quad x\in J_k^c,\quad (18)$$

$$\sigma_{1,2}(x,0)=\frac{2G\pi(1+\mathrm{tg}^2(\pi x/d))}{d(1+\kappa)}\mathrm{tg}\left(\frac{\pi x}{d}\right)\sqrt{\mathrm{tg}^2\left(\frac{\pi c}{d}\right)-\mathrm{tg}^2\left(\frac{\pi x}{d}\right)}\left(\frac{3r_0\mu}{\mathrm{tg}^3(\pi b/d)}+\right.$$

$$\left.+\frac{d(1+\kappa)(q_n-\mu p_n)}{2G\pi\left(1+\mathrm{tg}^2(\pi x/d)\right)}\cos\frac{\pi c}{d}\right)+\frac{6Gr_0\pi(1+\mathrm{tg}^2(\pi x/d))}{d(1+\kappa)\,\mathrm{tg}(\pi b/d)}\left(\frac{1}{2}-\frac{\mathrm{tg}^2(\pi x/d)}{\mathrm{tg}^2(\pi b/d)}\right)-\frac{p_n}{2}\pm\tau_{\max}(x,0),\quad x\in I_k^c,$$

$$\sigma_{1,2}(x,0)=\frac{6Gr_0\pi\cos^{-2}(\pi x/d)}{d(1+\kappa)\,\mathrm{tg}(\pi b/d)}\left(\left|\frac{\mathrm{tg}(\pi x/d)}{\mathrm{tg}(\pi b/d)}\right|\sqrt{\frac{\mathrm{tg}^2(\pi x/d)}{\mathrm{tg}^2(\pi b/d)}-1}-\frac{\mathrm{tg}^2(\pi x/d)}{\mathrm{tg}^2(\pi b/d)}+\frac{1}{2}\right)-\frac{p_n}{2}\pm\tau_{\max}(x,0),x\in J_k^b,$$

$$\sigma_{1,2}(x,0)=\frac{6Gr_0\pi(1+\mathrm{tg}^2(\pi x/d))}{d(1+\kappa)\,\mathrm{tg}(\pi b/d)}\left(\frac{1}{2}-\frac{\mathrm{tg}^2(\pi x/d)}{\mathrm{tg}^2(\pi b/d)}\right)-\frac{p_n}{2}\pm\tau_{\max}(x,0),\quad x\in J_k^{b,c}.\qquad (19)$$

In the formulas (19) the sign "+" refers to the σ_1, and the sign "-" refers to the σ_2.

The obtained analytical results are illustrated in Figs. 3–8, where the dimensionless parameters $\bar{x}=x/d$, $\bar{b}=b/d$, $\bar{r}_0=r_0/d$, $\bar{c}=c/d$, $\bar{q}_n=q_n/G$, $\bar{p}_n=p_n/G$, $\bar{\tau}_{\max}=\tau_{\max}/G$, $\bar{\sigma}_1=\sigma_1/G$, $\bar{\sigma}_2=\sigma_2/G$ are introduced. All the calculations were performed for the friction coefficient $\mu=0.3$, maximal depth of the groove $\bar{r}_0=10^{-4}$, Poisson ratio $\nu=0.2$, and nominal pressure $\bar{p}_n=5\cdot10^{-4}$.

The distributions of the principal shear stress $\bar{\tau}_{\max}$, the principal normal stresses $\bar{\sigma}_1$ and $\bar{\sigma}_2$ on the surface of the body D_1 for the half-width of groove $\bar{b}=0.2$ and the nominal tangential stress $\bar{q}_n=8.064\cdot10^{-5}$, which causes the initiation of the slip zone of the half-width $\bar{c}=0.15$, are given in Figs. 3–5 by the solid curve. The dashed curves correspond to full stick of the bodies (i.e. absence of slip). The solid vertical lines go through the edge of the slip zone, and the dashed vertical lines go through the edge of the groove. Fig. 3 shows that $\bar{\tau}_{\max}$ has two local maximums - one is located at the left edge of the slip zone and the other is located near the right edge of the slip zone. Besides, the latter exceeds the former. Therefore, for the textured bodies of plastic materials, the surface plastic yielding can begin within the slip zone near its right edge. It is interesting to note that the principal stress $\bar{\tau}_{\max}$ is constant throughout the surface when the full stick of the bodies is realized (the horizontal dashed line in Fig. 3). It means that the plastic body has the full-strength textured surface in the case of the absence of slip, i.e. the surface plastic yielding has not local character at the instant of its initiation, but covers the whole surface. In spite of the complete contact of bodies, the principal stress $\bar{\sigma}_1$ is tensile at a certain part of the groove, in particular within the slip zone (Fig. 4). The maximum value of $\bar{\sigma}_1$ is reached in the slip zone between its right edge and the groove center. Thus, for the textured brittle body the surface fracture due to the action of the tensile stress $\bar{\sigma}_1$ starts between the groove center and right edge of the slip zone. If the bodies are in stick, the maximum value of $\bar{\sigma}_1$ is reached at the center of the groove (the dashed line in Fig. 4). The principal stress $\bar{\sigma}_2$ is compressive on the whole surface of the textured body and its absolute maximal value is reached at the groove edges (Fig. 5). Therefore, in the case of the textured brittle body, zones located in the vicinity of the groove edges are sensitive to brittle fracture caused by the compressive stress. The principal stress $\bar{\sigma}_2$ in the case of frictional slip and the principal stress $\bar{\sigma}_2$ in the case of full stick are almost equal (the solid line and the dashed line match almost exactly in Fig. 5).

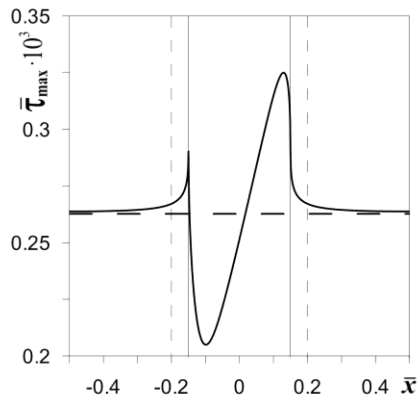

Fig. 3.

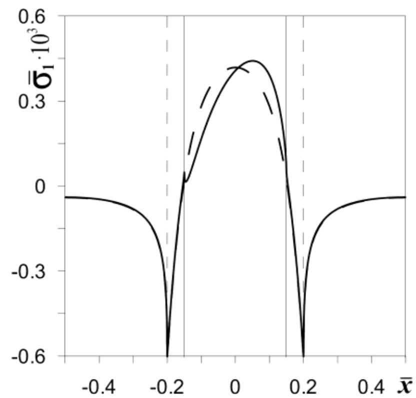

Fig. 4.

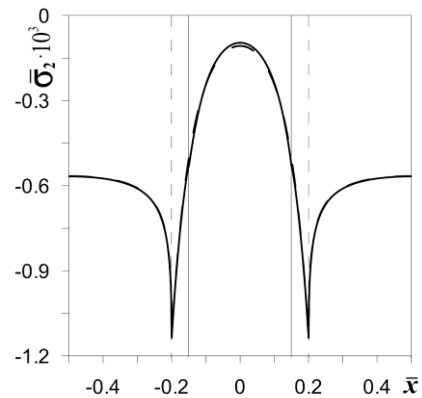

Fig. 5.

The distributions of the principal shear stress $\bar{\tau}_{max}$ (Fig. 6), the principal normal stress $\bar{\sigma}_1$ (Fig. 7), and the principal normal stress $\bar{\sigma}_2$ (Fig. 8) are obtained for the half-width of groove $\bar{b} = 0.3$ and different values of the nominal tangential stress $\bar{q}_n$: curve *1* corresponds to $\bar{q}_n = 9.276\cdot 10^{-5}$ ($\bar{c} = 0.2$), curve *2* corresponds to $\bar{q}_n = 1.071\cdot 10^{-4}$ ($\bar{c} = 0.25$), and curve *3* corresponds to $\bar{q}_n = 1.372\cdot 10^{-4}$ ($\bar{c} = 0.29$).

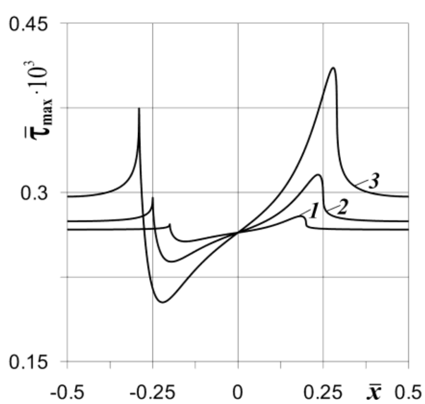

Fig. 6.

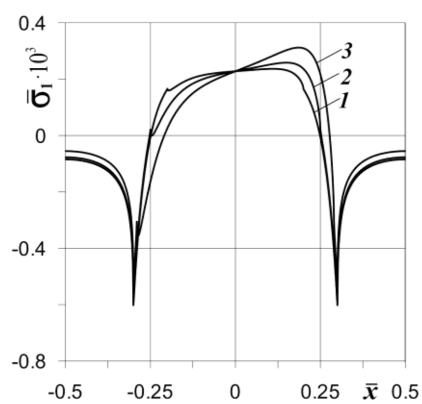

Fig. 7.

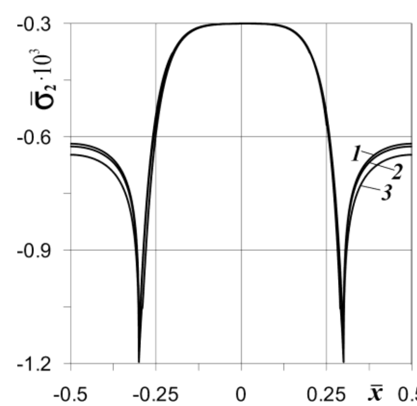

Fig. 8.

As the slip zone increases, the maximal values of the principal shear stress $\bar{\tau}_{max}$ increase, and the points where these maximal values are reached move rightward, but always are located within the slip zone (Fig. 6). Increase in the nominal tangential stress $\bar{q}_n$ leads to increase in the asymmetry of the principal stress $\bar{\sigma}_1$ distribution within the groove (Fig. 7). In so doing, the maximal values of $\bar{\sigma}_1$ reached near the right edge of the slip zone increase as the size of the slip zone increases. The principal stress $\bar{\sigma}_2$ is almost independent of the slip zone size (Fig. 8) and always reaches its absolute maximum at the groove edges.

It should be noted that the contact strength of bodies with single grooves was studied in [10].

Conclusions. The method for investigation of the contact interaction of two solids, one of which has a regular relief that is formed by a periodic system of shallow tunnel grooves of the same shape, under sequential loading by normal and shear forces is developed. This method is based on the method of the complex potentials. As a result, the corresponding problem is reduced to a singular integral equation with Hilbert kernel for the relative tangential shift of boundaries. For a certain shape of the groove, the analytical solution is obtained. By making use of the obtained analytical solution, the distributions of the principal normal and shear stresses on the surface of the textured body are analyzed. Based on the criterion of the maximum shear stress and the criterion of the maximum principal stress, it is shown that in brittle materials the most possible region of the cracks initiation is located between the groove center and groove edge when the material fails due to tensile normal stresses and at the groove edges when the material fails due to compressive normal stresses. For plastic materials, the plastic yielding necessarily occurs near the edges of the slip zone.

This work was supported by Russian Foundation for Basic Research (Grant No. 12-08-90434) and National Academy of Sciences of Ukraine (Grant No. 23-08-12).

References

[1] Nakano M., Korenaga Atsuko, Korenaga Atsushi, Miyake K., Murakami T., Ando Y., Usami H., Sasaki S. Applying micro-texture to cast iron surfaces to reduce the friction coefficient under lubricated conditions / Tribol Lett. Vol. 28. № 2. (2007), p. 131–137.

[2] Johnson K.L., Greenwood J.A., Higginson J.G. The contact of elastic regular wavy surfaces / Int. J. Mech. Sci. Vol. 27. № 6. (1985), p. 383–396.

[3] Kuznetsov Y.A., Gorokhovsky G.A. Stress distribution in a polymeric material subjected to action of a rough-surface indenter / Wear. Vol. 51. № 2. (1978), p. 299–308.

[4] Goryacheva I.G., in: *Mechanics of friction interaction*, edited by A. Yu. Ishlinsky / Nauka Publishing, Moscow (2001), 478 p.

[5] Shvets R.M., Martynyak R.M., Kryshtafovych A.A. Discontinuous contact of an anisotropic half-plane and a rigid base with disturbed surface / Int. J. Engng Sci. Vol. 34. № 2. (1996), p. 183–200.

[6] Kuznetsov Y.A., Gorokhovsky G.A. Friction interaction of a rough bodies from the point of view of mechanics of solids / Soviet Journal of Friction and Wear. Vol. 1. № 4. (1980), p. 638–649.

[7] Goryacheva I.G., Torskaya E.V. Modeling the contact wear fracture of a two-layer basement / Mech. Solids. Vol. 43. № 3. (2008), p. 426-436.

[8] Goryacheva I.G., Torskaya E.V. Modeling of fatigue wear of a two-layered elastic half-space in contact with periodic system of indenters / Wear. Vol. 268. № 11–12. (2010), p. 1417–1422.

[9] Kryshtafovych A.A., Martynyak R.M. Frictional contact of two elastic half-planes with wavy surfaces / J. Friction and Wear. Vol. 21. № 5. (2000), p. 1–8.

[10] Kryshtafovych A., Martynyak R. Strength of a system of mated anisotropic half-planes with surface recesses / Int. J. Eng. Sci. Vol. 39. (2001), p. 403–413.

[11] Muskhelishvili N.I., in: *Singular integral equations*, Noordhoff, Groningen, 1953.